Brownian Dynamics Simulations on the Self-Assembly Behavior of AB Hybrid Dendritic−Star Copolymers

Costas Georgiadis, Othonas Moultos, Leonidas N. Gergidis, and Costas Vlahos*

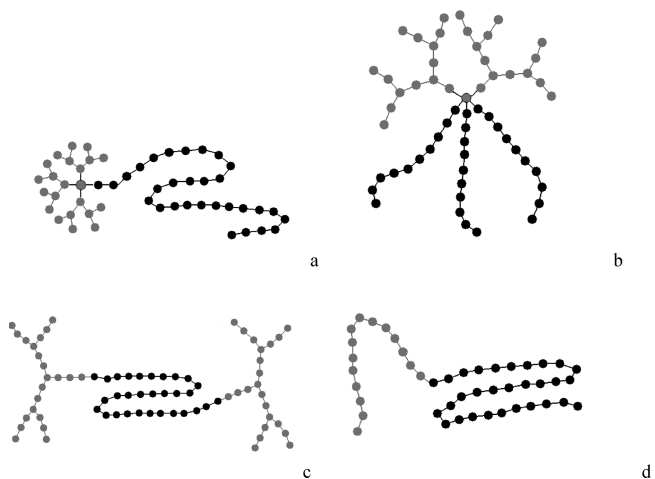*Department of Chemistry, University of Ioannina, 45110 Ioannina, Greece*

Received October 18, 2010. Revised Manuscript Received December 6, 2010

The micellization behavior of hybrid dendritic−star copolymers with solvophilic dendritic units is studied by means of Brownian dynamics simulations. The critical micelle concentration and the micelle size and shape are examined for different solvophobic/solvophilic ratios r as a function of the number of the dendritic and linear arms. Hybrid dendritic−star copolymers with one dendritic and up to three solvophobic linear branches form spherical micelles with preferential aggregation number. Those with two dendritic arms and three solvophobic branches form micelles with wide aggregation numbers only for small values of r. For hybrid dendritic−star copolymers with three dendritic arms and two or three solvophobic linear arms, micelles with wide aggregation numbers are also formed but for slightly higher values of r. Our results for the aggregation number are compared with existing results of other architectures obtained at the same temperature, and an inequality for the aggregation number is proposed.

1. Introduction

In a preceding paper we presented a systematic simulation study using the off-lattice Monte Carlo method on the conformational properties of AB hybrid dendritic−star copolymers[1] (Figure 1a,b) in an effort to describe how the mixing of the two different architectures influences the properties of the new macromolecule. The conditions under which the star branches' free ends concentrate at distance smaller than, equal to, or higher than the square root of the mean square radius of gyration of the dendritic part were defined for different solvent conditions. We also found that the number and the length of the star branches have a small effect on the conformation of the dendrimer block. In contrast, the micellization behavior of the dendrimer copolymer, which is the scope of the present study, is greatly influenced by the presence of linear chains attached to the central unit of the dendrimer leading to the formation of more complex, supramolecular assemblies in selective solvents.[2]

Recently, amphiphilic AB dendritic−linear block copolymers have emerged as a new class of amphiphilic copolymers with potential applications ranging from drug delivery and gene therapy to molecular templating.[3−6] The synthetic pathway of these block copolymers permits low polydispersity and full control over the molecular architecture. Dendritic−linear copolymers, synthesized and tested as drug carriers,[7] are composed

Figure 1. Cartoon representations of (a) hybrid dendritic−star copolymer $D_3G_2S_1(B_{30})_1$, (b) hybrid dendritic−star copolymer $D_2G_2S_2(B_{10})_3$, (c) dendritic−linear−dendritic $D_1G_2S_3(B_{30})_1D_1G_2S_3$, and (d) linear diblock copolymer $A_{15}B_{30}$.

from a hydrophobic[8] or hydrophilic[9] dendritic block attached to a linear block that has the opposite character. In the first case, the dendritic block forms the micelle core while the linear block faces the aqueous media. Because of the free volume interior regions of the dendritic cores, these micelles have the potential to store more hydrophobic drug molecules than the respective micelles of amphiphilic linear diblock copolymers. The other case, in which the dendritic block forms the micelles corona, is also very interesting because of the large number of free ends characterizing the dendritic architecture. The functionalization of these ends with targeting ligands (such as folic acid) dramatically increases the binding affinity of the dendritic−linear micelles on tumor cells.[10]

The effects of the dendritic architecture in the micellization properties of dendritic−linear copolymers were studied systematically by means of Brownian dynamics simulations adopting

---

*To whom correspondence should be addressed. E-mail: cvlahos@cc.uoi.gr.

(1) Gergidis, L.; Moultos, O.; Georgiadis, C.; Kosmas, M.; Vlahos, C. *Polymer* **2009**, *50*, 328–335.

(2) Frauenrath, H. *Prog. Polym. Sci.* **2005**, *30*, 325–384.

(3) Frechet, J. M. J.; Tomalia, D. A. *Dendrimers and Other Dendritic Polymers*; Wiley: New York, 2001.

(4) Patri, A. K.; Majoros, I. J.; Baker, J. R. *Curr. Opin. Chem. Biol.* **2002**, *6*, 466–471.

(5) Gitsov, I. Linear−dendritic block copolymers. Synthesis and characterization. In *Advances in Dendritic Macromolecules*; Newkome, G. R., Ed.; Elsevier Science: Amsterdam, 2002; Vol. *5*, pp 45−87.

(6) Grinstaff, M. W. *Chem.—Eur. J.* **2002**, *8*, 2838–2846.

(7) Gillies, E.; Frechet, J. *Bioconjugate Chem.* **2005**, *16*, 361–368.

(8) Gillies, E.; Jonsson, T.; Frechet, J. *J. Am. Chem. Soc.* **2004**, *126*, 11936–11943.

(9) Roman, C.; Fischer, H. R.; Meijer, E. W. *Macromolecules* **1999**, *32*, 5525–5531.

(10) Quitantana, A.; Raczka, E. L.; Lee, I.; Myc, A.; Majoros, I.; Patri, A.; Thomas, T.; Mule, J.; Baker, J. *Pharm. Res.* **2002**, *19*, 1310–1316.

bead−spring and freely joined chain models.[11,12] For solvophobic dendritic monomers, it was found[12] that the dendritic−linear copolymers form spherical micelles, with the preferential aggregation number being almost half compared with the respective linear diblock copolymer having the same total molecular weight and solvophobic-to-solvophilic ratio. The critical micelle concentration (cmc) of the dendritic−linear copolymer was found to be much higher than that of the linear diblock copolymers. For dendritic−linear copolymers with solvophilic dendritic beads and solvophobic linear block, it was found[11] that the cmc increases with the dendron generation for a fixed dendritic architecture. This increase was shown to be higher than what would be expected for a traditional diblock copolymer. Comparing dendritic−linear copolymers with the same molecular weight and solvophobic-to-solvophilic ratio, it was found that cmc decreases as the number of spacer monomers between branching points in the dendron increases. The micelles aggregation number can be controlled by changing the dendron generation and spacer length. The dendritic block forms a solvophilic corona, which resides in higher density regions around the core in comparison with the linear diblock copolymer.

The micellization behavior and properties of hybrid dendritic−star copolymers with solvophilic dendritic beads is expected to be more exciting since the cmc, the aggregation number, and the density of the dendritic corona would be controllable by changing the number of dendritic and linear blocks.[13] Moreover, the dendritic−star copolymers exhibit some similarities with the star block copolymers, which form micelles with morphology different from typical micelles, such as connected star aggregates, segmented worm, and core-lump.[14] The reason is that the dense solvophilic dendritic part of a single dendritic−star chain which consists the core of the molecule, exposes the solvophobic linear branches to the periphery as in the star block chains. Depending on the number and the length of linear blocks, one, two or three aggregative domains can be formed on the outer rim of the solvophilic dendritic blocks. One aggregative domain leads to the formation of spherical micelles, two aggregative domains leads to the segmented worm-like architecture, and three leads to the connected star micelles. The hybrid dendritic−star copolymer architecture can be also useful in order to describe the hyperbranched linear polyethylenes in various solvent conditions.[15]

We employed Brownian dynamics simulations in order to elucidate the effects of the hybrid dendritic−star architecture on the micellization behavior. The properties of interest are the cmc, the mean aggregation number, the shape of the micelle which is expressed by the shape anisotropy k^2, the thickness of the corona H, and the solvophobic core radius R_c. In addition, we report comparisons of our simulation results with simulation studies of dendritic−linear, traditional linear diblock, and H-shaped copolymers existing in the literature.[11,16]

2. Model

We employed a coarse-grained model to represent the amphiphilic copolymers. A group of atoms was modeled as a bead (with diameter σ), while different beads were connected with flexible

finitely extended elastic bonds (FENE). The FENE potential is expressed as

$$U_{\text{Bond}}(r_{ij}) = \begin{cases} -0.5kR_0^2 \ln\left[1 - \left(\dfrac{r_{ij}}{R_0}\right)^2\right], & r_{ij} \leq R_0 \\ \infty, & r_{ij} > R_0 \end{cases} \quad (1)$$

where r_{ij} is the distance between beads i and j, $k = 25T\varepsilon/\sigma^2$, and R_0 is the maximum extension of the bond ($R_0 = 1.5\sigma$). These parameters[17] prevent chain crossing by ensuring an average bond length of 0.97σ. Monomer−monomer interactions were calculated by means of a truncated and shifted Lennard-Jones potential:

$$U_{\text{LJ}}(r_{ij})$$
$$= \begin{cases} 4\varepsilon_{ij}\left[\left(\dfrac{\sigma}{r_{ij}}\right)^{12} - \left(\dfrac{\sigma}{r_{ij}}\right)^6 - \left(\dfrac{\sigma}{r_{cij}}\right)^{12} + \left(\dfrac{\sigma}{r_{cij}}\right)^6\right] + \varepsilon_{ij}, & r_{ij} \leq r_{cij} \\ 0, & r_{ij} > r_{cij} \end{cases}$$
$$(2)$$

where ε_{ij} is the well-depth, and r_{cij} is the cutoff radius. The solvent molecules are considered implicitly. The short timesteps needed to model the solvent behavior (the fast motion) restrict the time scales that maybe sampled, thereby limiting the information that can be obtained for the slower motion of the copolymer. The Brownian dynamics simulation method allows the statistical treatment of the solvent, incorporating its influence on the copolymer by a combination of random forces and frictional terms. The friction coefficient and the random force couple the simulated system to a heat bath, and therefore the simulation has canonical ensemble (NVT) constraints. The equation of motion of each bead i of mass m in the simulation box follows the Langevin equation:

$$m_i\ddot{\mathbf{r}}_i(t) = -\nabla\sum_j[U_{\text{LJ}}(r_{ij}) + U_{\text{Bond}}(r_{ij})] - m_i\xi\dot{\mathbf{r}}_i(t) + \mathbf{F}_i(t) \quad (3)$$

where m_i, $\mathbf{r}_i$, and ξ are the mass, the position vector, and the friction coefficient of the i bead, respectively. The friction coefficient is equal to $\xi = 0.5\tau^{-1}$, with $\tau = \sigma(m/\varepsilon)^{1/2}$. The random force vector $\mathbf{F}_i$ is assumed to be Gaussian, with zero mean, and satisfies the equation

$$\langle\mathbf{F}_i(t)\cdot\mathbf{F}_j(t')\rangle = 6k_{\text{B}}Tm\xi\delta_{ij}\delta(t-t') \quad (4)$$

where k_{B} is the Boltzmann constant and T is the temperature.

Some of the polymer molecules simulated in this work are illustrated in Figure 1. The hybrid dendritic−star copolymers contain one (D_1), two (D_2), or three (D_3) solvophilic dendritic blocks of the first (G_1), second (G_2), or third (G_3) generation with spacer length one (S_1), two (S_2), or three (S_3) beads. All dendritic beads are of type A and considered solvophilic. In all conducted simulations, the solvophobic part B of copolymers contains 30 beads. In the case of hybrid dendritic−star copolymers, the solvophobic B units are distributed in one $(B_{30})_1$, two $(B_{15})_2$, or three $(B_{10})_3$ branches with 30, 15, and 10 units, respectively. For comparison purposes, linear diblock copolymers $A_{N_1}B_{30}$, with N_1 solvophilic beads, and dendritic−linear−dendritic ABA triblock copolymers $D_1G_2S_1(B_{30})D_1G_2S_1$, $D_1G_2S_3(B_{30})D_1G_2S_3$ are also simulated.

The Brownian dynamics simulations were performed in a cubic box with periodic boundary conditions, using the open-source massive parallel simulator LAMMPS.[18,19] Previous works have

(11) Suek, N.; Lamm, M. *Langmuir* **2008**, *24*, 3030–3036.
(12) Cheng, L.; Cao, D. *Langmuir* **2009**, *25*, 2749–2756.
(13) Wurm, F.; Frey, H. *Prog. Polym. Sci.* [Online early access]. DOI: 10.1016/j.progpolymsci 2010.07.009.
(14) Sheng, Y.; Nung, C.; Tsao, H. *J. Phys. Chem. B* **2006**, *110*, 21643–21650.
(15) Xu, Y.; Xiang, P.; Ye, Z.; Wang, W. J. *Macromolecules* **2010**, *43*, 8026–8038.
(16) Moultos, O.; Gergidis, L.; Vlahos, C. *Macromolecules* **2010**, *43*, 6903–6911.

(17) Murat, M.; Grest, G. *Macromolecules* **1996**, *29*, 1278–1285.

proven the high efficiency of LAMMPS in the study of amphiphilic copolymers.[11,12,16] Different cutoff values in the Lennard-Jones potential were used[11,12,16] to describe the interactions between copolymer units with $\varepsilon_{ij} = \varepsilon$. The A−A and A−B interactions were considered repulsive and had cutoff radii of $r_{cij} = 2^{1/6}\sigma$, while the B−B had an attractive potential with cutoff radius $r_{cij} = 2.5\sigma$. For the sake of simplicity, all beads A, B, and C were considered to have the same mass ($m = 1$) and diameter ($\sigma = 1$).

In this work, system sizes with 125 and 1000 polymeric chains were simulated. Amphiphiles were assumed to reside to the same micelle if the distance between any two nonbonded solvophobic beads B, belonging to different chains, was found to be within 1.5σ. The aforementioned criterion has been adopted by the literature for the description of the micellization process where this distance corresponds to the maximum extension of the FENE bonds.[11,12,16] The reduced temperature of the simulation T^* was set to $T^* = k_B T/\varepsilon = 1.8$. This choice of temperature allows the studied systems to have both micelles and free molecules.[11] If the temperature is very low, the studied system contains only aggregates and no free molecules, while if the temperature is very high, the studied system contains only free molecules and no aggregates. The system size was chosen so to prevent the largest micelles from having a radius of gyration greater than one-fourth of the box side length. For this particular reason we have used detailed exploratory runs with various simulation box sizes for low and high densities ensuring that every system studied shows identical aggregate size distributions. The use of the one-quarter of the simulation box side proved to be a sufficient condition to avoid interaction of chains and micelles with their images. No system size effects were observed for all the calculated quantities reported on this paper. In all simulations, we set $\varepsilon = 1$.

In order to avoid bond crossing at the desired concentration, the AB or the ABA copolymer molecule was arranged on a lattice box. The energy of the chain was minimized, and then the small system was replicated N_{Polymer} times, equal to the number of polymer chains. We performed one million time steps with time step $\Delta t = 0.008\tau$ setting all cutoff radii equal to $r_{cij} = 2^{1/6}\sigma$ in order to eliminate any bias introduced from the initial conformation. The system then was allowed to equilibrate for five million steps. The simulation subsequently conducted for 15 million steps for the 125 polymer chains, and up to 50 or 60 million steps for larger systems with 1000 chains. The length of the simulation was evaluated by calculating the tracer autocorrelation function:

$$C(t) = \frac{\langle N(t_0 + t)N(t_0)\rangle - \langle N(t_0)\rangle^2}{\langle N^2(t_0)\rangle - \langle N(t_0)\rangle^2} \tag{5}$$
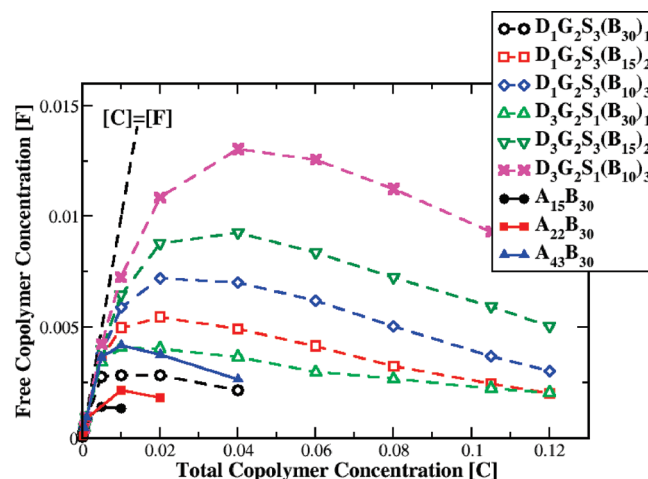
where $N(t)$ is the number of molecules in the micelle in which the copolymer resides at time t. We took all copolymers as tracers, and every time step as a time origin t_0. The characteristic relaxation time t_c is defined as the required time for $C(t)$ to reach the value of e^{-1}. Each simulation was run at least $10t_c$ to have 10 independent conformations. The properties of interest were calculated as averages from 1500 and 5000 snapshots for the systems, with 125 and 1000 chains, respectively.
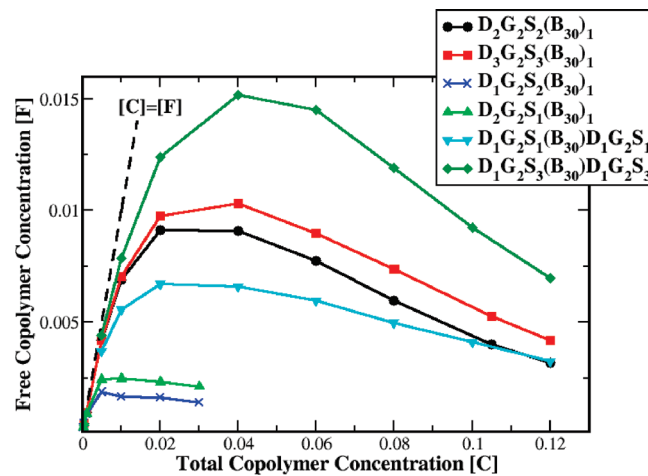
3. Results and Discussion

A. Critical Micelle Concentration. The driving force of the micelle formation of the copolymers in a selective solvent at constant temperature is the free energy difference per chain

(18) LAMMPS Molecular Dynamics Simulator http://lammps.sandia.gov. Accessed 12/2010.

(19) Plimpton, S. *J. Comput. Phys.* **1995**, *117*, 1–19.

Figure 2. Concentration of the free copolymers [F] versus the total copolymer concentration [C] for various hybrid dendritic−star copolymers and linear diblock copolymers.

Figure 3. Concentration of the free copolymers [F] versus the total copolymer concentration [C] for hybrid dendritic−star and dendritic−linear−dendritic copolymers.

between the free chain in the solution and the chain in the aggregate. In a particular concentration called the cmc, there is an abrupt increase in the fraction of chains involved in the formation of micelles. The cmc is an important property of self-assembly because it is a direct measure of the thermodynamic stability of the micelles in the solution. The onset of micellization is traditionally depicted by plotting the free (nonassociated) copolymer monomers concentration [F] as a function of the total copolymer monomers concentration [C]. The total copolymer concentration is defined as $[C] = N_w n/V$, where n is the number of copolymer molecules, N_w is the number of monomer beads per copolymer molecule, and V is the total volume of the simulation box. The maximum concentration [F] defines the cmc for the system. More or less, at the cmc, 5% of the mole fraction of amphiphilic copolymers are contained in micelles.[20]

Figures 2 and 3 show plots of the free copolymer concentration against the total copolymer concentration for the simulated dendritic−star, dendritic−linear, dendritic−linear−dendritic, and traditional AB linear copolymers. The cmc values calculated from Figures 2 and 3 are given in Table 1. The molecular theory

(20) Tanford, C. *J. Phys. Chem.* **1974**, *78*, 2469–2479.

Table 1. CMC for Different Dendritic−Star, Dendritic−Linear−Dendritic and Linear Diblock Copolymers

architecture	MW	cmc	r
$D_1G_2S_3(B_{30})_1$	52	0.0029	1.36
$D_1G_2S_3(B_{15})_2$	52	0.0055	1.36
$D_1G_2S_3(B_{10})_3$	52	0.0072	1.36
$D_3G_2S_1(B_{30})_1$	52	0.0041	1.36
$D_3G_2S_1(B_{15})_2$	52	0.0093	1.36
$D_3G_2S_1(B_{10})_3$	52	0.013	1.36
$A_{22}B_{30}$	52	0.0022	1.36
$D_1G_2S_2(B_{30})_1$	45	0.0019	2.0
$D_2G_2S_1(B_{30})_1$	45	0.0025	2.0
$D_1G_2S_1(B_{30})D_1G_2S_1$	44	0.0067	2.1
$A_{15}B_{30}$	45	0.0014	2.0
$D_2G_2S_3(B_{30})_1$	73	0.0091	0.7
$D_3G_2S_2(B_{30})_1$	73	0.0103	0.7
$D_1G_2S_3(B_{30}) D_1G_2S_3$	74	0.0152	0.68
$A_{43}B_{30}$	73	0.0042	0.7

for the formation of micelles can be used to qualitatively describe the trends of these values. According to the theory, the mole fraction of micelles X_n with an aggregation number n is equal to

$$X_n = X_1 \exp(-g_{mic}/k_B T) \qquad (6)$$

and inversely proportional to the cmc.[21] X_1 is the mole fraction of unimers, and g_{mic} is the change in the Gibbs free energy associated with the transfer of n unimers from the solution to a micelle. This free energy for uncharged copolymers can be modeled as the sum of four different terms that takes into account all of the free energy changes that occur upon micelle formation:[21] $g_{mic} = g_{tr} + g_{int} + g_{pack} + g_{st}$. The first three terms are related to the solvophobic part of the copolymer, and the fourth is associated with the solvophilic counterpart. The free energy of transfer g_{tr} reflects the energy change associated with the transfer of the solvophobic block from the solution to micelles core. The interfacial free energy g_{int} takes into account the energy change upon the formation of the interface between the core and the solution, while g_{pack} involves the free energy change associated with constraining the end or ends of the solvophobic part to lie at the periphery of the micelle core. The last term g_{st} accounts for the contribution of steric interactions between the solvophilic units of the copolymers.

Table 1 shows that, for dendritic−star copolymers containing one solvophilic dendron of second generation with spacer length three, having one, two, or three solvophobic linear arms ($D_1G_2S_3$-$(B_{30})_1$, $D_1G_2S_3(B_{15})_2$, $D_1G_2S_3(B_{10})_3$) with lengths 30, 15, and 10 respectively, the cmc values are proportional to the number of linear arms. The reason is the different interfacial energy per chain g_{int} needed from these copolymers in the process of aggregation. In the case of copolymer $D_1G_2S_3(B_{30})_1$ the long solvophobic arm could extend far away from the connection point with the dendritic head, thus reducing the interface with the solvent and consequently the enthalpic interactions with the solvent. Moreover, the extension of the large arm increases the interface exposed to other copolymers' solvophobic arms, resulting in a higher probability of interaction with them and, furthermore, reducing the free energy of the copolymer.[12]
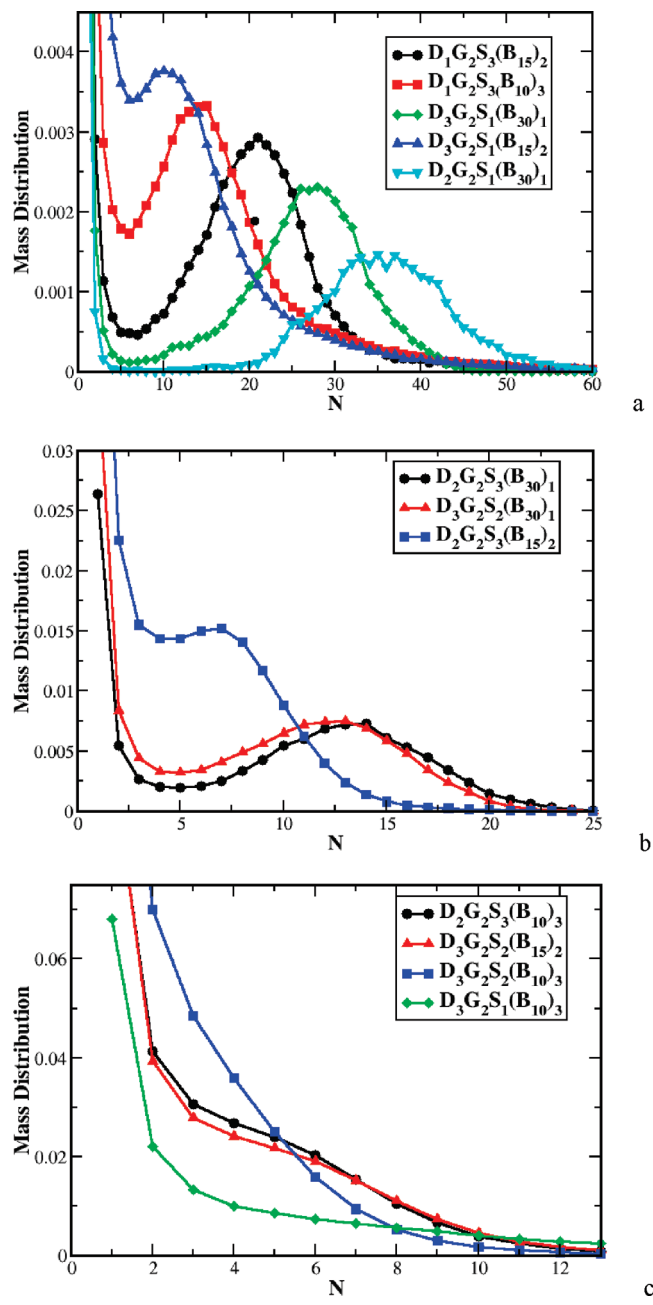
In the case of $D_1G_2S_3(B_{15})_2$ copolymer with two shorter arms, many units are constrained near the point of connection with the dendritic head. Thus, a creation of a larger interface, with the solvent molecules, leads to a larger interfacial energy and consequently to a higher cmc value according to eq 6. Furthermore, the concentration of the units close to the point of connection hinders

their interaction with other solvophobic units in order to further reduce the free energy.[12] The cmc value for $D_1G_2S_3(B_{15})_2$ is slightly smaller than twice the one for $D_1G_2S_3(B_{30})_1$, and the respective cmc value for $D_1G_2S_3(B_{10})_3$ is smaller than the one for $D_1G_2S_3(B_{30})_1$ copolymers tripled.

The rise in the cmc with the increase of solvophobic arms is more effective in the case of hybrid dendritic−star copolymers containing three dendritic branches. The $D_3G_2S_1(B_{30})_1$, $D_3G_2S_1$-$(B_{15})_2$, $D_3G_2S_1(B_{10})_3$ copolymers have the same molecular weight with the previous copolymers, but the spacer length is smaller, making the dendrons very stiff with the majority of the solvophilic beads concentrated around the micelle interface. The steric interactions between units of different copolymer chains in this case are higher than the steric interactions of the $D_1G_2S_3$ dendrons, leading to larger cmc values (0.0041, 0.0093, 0.0130) for the $D_3G_2S_1$-$(B_{30})_1$, $D_3G_2S_1(B_{15})_2$, $D_3G_2S_1(B_{10})_3$ copolymers, respectively. The rise in the cmc value is not the same if we increase the number of dendritic arms from one to two and from two to three. Our results for the couples $D_1G_2S_2(B_{30})_1$, $D_2G_2S_1(B_{30})_1$ with molecular weight 45 and $D_2G_2S_3(B_{30})_1$, $D_3G_2S_2(B_{30})_1$ containing 73 beads indicates that the cmc value is higher in the second case. This happens because higher steric penalties are introduced, making the transfer of the copolymer chain with three stiff dendrons in the micelles corona more difficult.

In addition to the molecular theory of micellization for linear copolymers, it was found that the cmc depends on the solvophobic/solvophilic molecular weight ratio r.[11] The increase of the ratio r leads to a monotonic decrease of the cmc. In the copolymers studied in this work, as can be observed in Table 1, the aforementioned trend is valid only if we compare copolymers with the same number of solvophobic arms. The reason is the different interfacial energy associated with the formation of the micelles in copolymers with a different number of solvophobic arms. For comparison purposes, we have also simulated traditional linear diblock copolymers and the dendritic−linear−dendritic[22] $D_1G_2S_1$-$(B_{30})D_1G_2S_1$, $D_1G_2S_3(B_{30})D_1G_2S_3$ triblock copolymers. In the latter case, the two dendrons are connected to the opposite ends of the linear solvophobic bridge and are identical to the respective dendrons of $D_2G_2S_1(B_{30})_1$ and $D_2G_2S_3(B_{30})_1$ hybrid dendritic−star copolymers. The cmc values found are also listed in Table 1. It can be observed that the linear diblock copolymers have the lowest cmc value among copolymers with the same ratio r and the same total molecular weight. This is due to the small steric penalty needed to be overcome for transferring the linear chains from the solution to the micelle. Closer to the cmc values of linear copolymer are the respective ones of dendritic copolymers with one linear and one dendritic arm. The cmc of dendritic−linear−dendritic copolymers is twice the cmc value of the respective dendritic copolymer and consequently close to the cmc value of the dendritic−star containing two solvophilic dendrons and two solvophobic linear arms. According to the molecular theory of micellization, the free energy g_{pack} associated with constraining both ends of the solvophobic bridge to lie in the periphery in dendritic−linear−dendritic copolymers is higher than the free energy change associated with constraining the one end of the solvophobic part in dendritic−linear copolymers. The reported values for the cmc of $A_{15}B_{30}$ and $D_1G_2S_2(B_{30})_1$ are systematically lower than the values for the cmc reported by ref 11 for similar architectures with molecular weight equal to 45. These differences may be attributed to a subtle difference in the model or simulation parameters.

(21) Nagarajan, R. *Langmuir* **1985**, *1*, 331–341.

(22) Nguyen, P.; Hammond, P. *Langmuir* **2006**, *22*, 7825–7832.
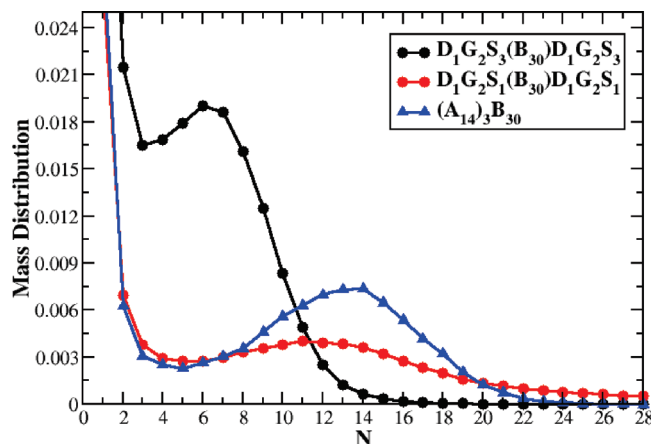
Figure 4. Mass distribution of the aggregates for various hybrid dendritic−star copolymers: (a,b) aggregates following a bell-shaped distribution and (c) aggregates following a non-bell-shaped distribution.

B. Micelle Size and Shape. The aggregation number, the radii of gyration of the solvophobic and solvophilic parts and of the whole aggregate, as well as the resulting shape anisotropy k^2 are useful tools for characterizing the micelles formed by amphiphilic copolymers. Shape anisotropy is defined as[11,23]

$$\kappa^2 = 1 - 3\frac{\langle I_2 \rangle}{\langle I_1^2 \rangle} \tag{7}$$

where I_1 and I_2 are the first and second invariants of the radius of gyration tensor. $k^2 = 0$ corresponds to a perfect sphere, while $k^2 = 1$ corresponds to a perfect rod. All these properties were calculated on the most concentrated system having $[C] = 0.12$

(23) Theodorou, D. N.; Suter, U. W. *Macromolecules* **1985**, *18*, 1206–1214.

Figure 5. Mass distribution of the aggregates for dendritic−linear−dendritic and miktoarm star copolymers.

where most aggregates are formed. Figures 4 and 5 show our results on the mass distribution of the aggregates for various hybrid dendritic−star and dendritic−linear−dendritic copolymers.

However, some of our results can be directly compared with respective simulation findings of refs 11 and 16 concerning the micellization properties of linear diblock, dendritic−linear, and H-shaped copolymers. Linear, linear−dendritic, and H-shaped copolymers contain 30 solvophobic units, and their micellalization behavior was studied at the reduced temperature $T^* = 1.8$, also used in our simulations. The preferential aggregation number and the shape characteristics of our results are listed in Tables 2 and 3, while some results of refs 11 and 16 are presented in Table 4. It can be observed that between copolymers with different architecture but with similar molecular weight ($M_w = 45$) and solvophobic/solvophilic ratio ($r = 2$), the preferential aggregation number follows the inequality $N_{\text{p linear A15B30}} > N_{\text{p linear−dendritic D1G2S2 B30}} > N_{\text{p linear−dendritic D1G3S1B30}} > N_{\text{p dendritic−star D2G2S1B30}} > N_{\text{p star (A4)4B30}} > N_{\text{p dendritic−linear−dendritic D1G2S1(B30)D1G2S1}} > N_{\text{p H-shaped (A4)2B30(A4)2}}$. This inequality reflects the difference in steric interactions between solvophilic units in the corona, and the change in the free energy g_{pack}, associated with constraining the end or both of the solvophobic parts to lie on the periphery of the micelle core. Among the dendritic copolymers, the dendritic−linear copolymers of second generation, $D_1G_2S_2(B_{30})_1$, form micelles with higher aggregation number $N_p = 47$. The increase of dendron generation greatly decreases the aggregation number ($N_p = 38$) while the addition of another dendron $D_2G_2S_1(B_{30})_1$ further reduces the N_p ($N_p = 35$). The most dramatic decrease of N_p, in dendritic copolymers, is observed in the case of dendritic−linear−dendritic $D_1G_2S_1$-$(B_{30})D_1G_2S_1$ ($N_p = 11$) indicating that the contribution of the packing free energy g_{pack} plays a predominant role in the aggregation phenomena of copolymers.

The micelle core shape anisotropy k^2_{core} for linear, dendritic−linear of second and third generation, hybrid dendritic−star, and miktoarm star copolymers has equal values within the standard deviation, while the respective value for the H-shaped copolymers is higher. The highest value of k^2_{core} observed for the dendritic−linear−dendritic architecture indicates a less spherical topology. As far as the total micelle shape anisotropy k^2_{micelle} is concerned, one can observe that the most spherical micelles are formed by linear diblock copolymers. Dendritic−linear and hybrid dendritic−star copolymers have the same k^2_{micelle} values, while H-shaped and dendritic−linear−dendritic copolymers show increasing deviation from the spherical topology.

Table 2. Shape Characteristics of the Most Probable Aggregates Formed by Hybrid Dendritic−Star, Dendritic−Linear−Dendritic and Miktoarm Star Copolymers[a]

copolymer	M_w	N_p	$\langle R_g^2 \rangle_{micelle}$	$\langle R_g^2 \rangle_{core}$	$\langle R_g^2 \rangle_{corona}$	H	R_c
$D_1G_2S_3(B_{15})_2$	52	21	54.7 (0.4)	32.4 (0.4)	84.7 (0.3)	2.191	7.354
$D_1G_2S_3(B_{10})_3$	52	15	47.3 (0.2)	30.6 (0.3)	69.6 (0.2)	1.731	7.146
$D_3G_2S_1(B_{30})_1$	52	26	59.2 (0.2)	34.7 (0.2)	92.2 (0.2)	2.322	7.608
$D_3G_2S_1(B_{15})_2$	52	10	36.0 (0.2)	25.3 (0.2)	50.2 (0.2)	1.217	6.524
$D_2G_2S_1(B_{30})_1$	45	35	59.6 (0.3)	40.0 (0.3)	98.5 (0.3)	1.802	8.162
$D_2G_2S_3(B_{30})_1$	73	14	64.4 (0.1)	25.0 (0.1)	91.5 (0.1)	3.907	6.454
$D_2G_2S_3(B_{15})_2$	73	7	42.1 (0.1)	18.9 (0.1)	57.8 (0.1)	2.772	5.606
$D_3G_2S_2(B_{30})_1$	73	13	60.4 (0.1)	25.3 (0.1)	84.4 (0.1)	3.534	6.496
$(A_{14})_3B_{30}$	72	14	66.1 (0.2)	25.6 (0.2)	94.6 (0.2)	3.960	6.537
$D_1G_2S_3(B_{30}) D_1G_2S_3$	74	6	51.0 (0.2)	37.9 (0.1)	59.4 (0.2)	1.273	7.948
$D_1G_2S_1(B_{30})D_1G_2S_1$	44	11	37.4 (0.3)	30.5 (0.3)	52.1 (0.3)	0.773	7.127

copolymer	$\langle k^2 \rangle_{micelle}$	$\langle k^2 \rangle_{core}$	$\langle R_g^2 \rangle_{free}$
$D_1G_2S_3(B_{15})_2$	0.061 (0.004)	0.139 (0.006)	9.93 (0.02)
$D_1G_2S_3(B_{10})_3$	0.092 (0.003)	0.187 (0.005)	8.84 (0.01)
$D_3G_2S_1(B_{30})_1$	0.041 (0.001)	0.076 (0.003)	9.71 (0.04)
$D_3G_2S_1(B_{15})_2$	0.111 (0.003)	0.181 (0.004)	7.22 (0.01)
$D_2G_2S_1(B_{30})_1$	0.040 (0.002)	0.069 (0.004)	9.00 (0.05)
$D_2G_2S_3(B_{30})_1$	0.043 (0.001)	0.100 (0.002)	14.06 (0.02)
$D_2G_2S_3(B_{15})_2$	0.078 (0.001)	0.181 (0.002)	11.79 (0.01)
$D_3G_2S_2(B_{30})_1$	0.048 (0.001)	0.103 (0.002)	12.19 (0.03)
$(A_{14})_3B_{30}$	0.040 (0.001)	0.096 (0.002)	15.88 (0.02)
$D_1G_2S_3(B_{30}) D_1G_2S_3$	0.148 (0.001)	0.229 (0.002)	18.14 (0.03)
$D_1G_2S_1(B_{30})D_1G_2S_1$	0.145 (0.002)	0.187 (0.003)	9.26 (0.03)

[a] Standard deviation is inside the parentheses.

Table 3. Shape Characteristics of Copolymers Forming Micelles with Widely Distributed Aggregation Number[a]

Copolymer	M_w	N_P	$\langle k^2 \rangle_{micelle}$	$\langle k^2 \rangle_{core}$	$\langle R_g^2 \rangle_{free}$
$D_3G_2S_1(B_{10})_3$	52	3	0.218 (0.001)	0.255 (0.002)	6.042 (0.004)
$D_3G_2S_1(B_{10})_3$	52	5	0.170 (0.002)	0.240 (0.002)	6.042 (0.004)
$D_3G_2S_1(B_{10})_3$	52	10	0.199 (0.003)	0.279 (0.003)	6.042 (0.004)
$D_3G_2S_1(B_{10})_3$	52	21	0.317 (0.005)	0.374 (0.005)	6.042 (0.004)
$D_2G_2S_3(B_{10})_3$	73	3	0.157 (0.001)	0.237 (0.001)	10.799 (0.007)
$D_2G_2S_3(B_{10})_3$	73	5	0.104 (0.001)	0.225 (0.002)	10.799 (0.007)
$D_2G_2S_3(B_{10})_3$	73	10	0.165 (0.003)	0.340 (0.005)	10.799 (0.007)
$D_3G_2S_2(B_{15})_2$	73	3	0.191 (0.001)	0.240 (0.001)	9.650 (0.005)
$D_3G_2S_2(B_{15})_2$	73	5	0.117 (0.001)	0.214 (0.002)	9.650 (0.005)
$D_3G_2S_2(B_{15})_2$	73	12	0.216 (0.005)	0.381 (0.009)	9.650 (0.005)
$D_3G_2S_2(B_{10})_3$	73	3	0.183 (0.001)	0.257 (0.001)	8.588 (0.003)
$D_3G_2S_2(B_{10})_3$	73	5	0.138 (0.002)	0.264 (0.002)	8.588 (0.003)
$D_3G_2S_2(B_{10})_3$	73	10	0.258 (0.003)	0.415 (0.005)	8.588 (0.003)
$D_3G_2S_2(B_{10})_3$	73	19	0.33 (0.04)	0.42 (0.04)	8.588 (0.003)

[a] $\langle R_g^2 \rangle_{free}$ is the radius of gyration of nonaggregated chains (standard deviation is inside the parentheses).
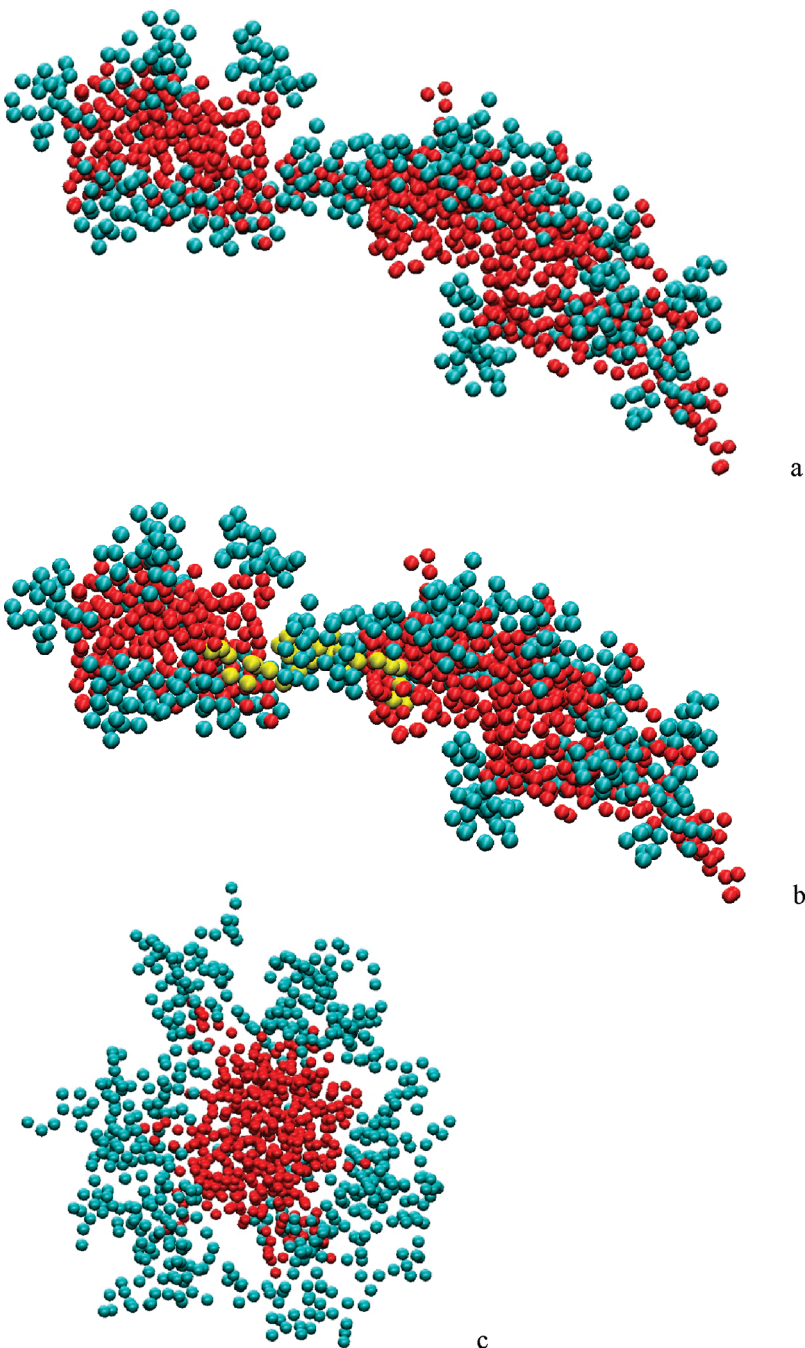
Table 4. Aggregation Number and Shape Characteristics of the Most Probable Aggregates Formed by Linear Diblock, Hybrid Dendritic−Linear, Dendritic−Star, Dendritic−Linear−Dendritic, Miktoarm Star, and H-Shaped Copolymers[a]

Copolymer	N_p	M_w	$\langle k^2 \rangle_{micelle}$	$\langle k^2 \rangle_{core}$	Reference
$A_{15}B_{30}$	62	45	0.029 (0.007)	0.064 (0.014)	11
$D_1G_2S_2B_{30}$	47	44	0.038 (0.007)	0.071 (0.011)	11
$D_1G_3S_1B_{30}$	38	45	0.038 (0.003)	0.065 (0.006)	11
$D_2G_2S_1B_{30}$	35	45	0.040 (0.002)	0.069 (0.004)	
$(A_4)_4B_{30}$	31	46	0.046 (0.002)	0.076 (0.003)	16
$D_1G_2S_1(B_{30})D_1G_2S_1$	11	44	0.145 (0.002)	0.187 (0.003)	
$(A_4)_2B_{30}(A_4)_2$	8	46	0.108 (0.002)	0.164 (0.003)	16

[a] Standard deviation is inside the parentheses.

In addition, we study the effects of the number of the solvophobic arms on the aggregation number of dendritic copolymers. We consider systems with two dendritic and one, two, or three solvophobic linear arms with total $M_w = 73$ and solvophobic/solvophilic ratio $r = 0.7$ ($D_2G_2S_3(B_{30})_1$, $D_2G_2S_3(B_{15})_2$, $D_2G_2S_3(B_{10})_3$). Our results are presented in Table 2. It can be observed that the dendritic copolymer with two solvophobic arms $D_2G_2S_3(B_{15})_2$ forms micelles with half the aggregation number ($N_p = 7$) compared to the respective dendritic copolymer with one solvophobic arm $D_2G_2S_3(B_{30})_1$ ($N_p = 14$). The reason is the different free energy of packing g_{pack} of the one and two solvophobic arms needed for the formation of the micelles core, explained in detail in the previous section referring to the cmc. Further increase in the number of solvophobic arms ($D_2G_2S_3(B_{10})_3$) leads to micelles with a wide range of aggregation numbers. The mass distribution of the aggregates in this case follows a non-bell-shaped distribution as can be observed in Figure 4c. The equivalent ($M_w = 73$, $r = 0.7$) hybrid dendritic−star copolymers with three dendritic arms and one solvophobic linear chain $D_3G_2S_2(B_{30})_1$ form

micelles with slightly lower aggregation number, $N_p = 13$ (Figure 4b), while the others, with two and three solvophobic arms, form micelles with a wide range of aggregation numbers (Figure 4c). Comparing with other architectures, we found that the dendritic−linear−dendritic copolymer $D_1G_2S_3(B_{30})D_1G_2S_3$ has the same aggregation number as the $D_2G_2S_3(B_{15})_2$. This finding indicates that the free energy of packing of the two solvophobic arms is almost similar to the corresponding energy of placing both ends of the solvophobic linear bridge of dendritic−linear−dendritic copolymer to lie at the micelles' core periphery. The equivalent miktoarm star $(A_{14})_3B_{30}$ copolymer with three solvophilic arms forms micelles with slightly higher aggregation number ($N_p = 14$) than the $D_3G_2S_2(B_{30})_1$ and the same with the $D_2G_2S_3(B_{30})_1$. The respective H-shaped copolymer $(A_{10})_2B_{30}(A_{10})_2$ forms micelles with no preferential aggregation number.[16]

The shape of the micelles of the dendritic copolymers in which the mass distribution of aggregates follows a bell-shaped distribution is more or less spherical, as can be observed from the $k^2_{micelle}$ values in Table 2. Also spherical are all the micelles with a wide range of aggregation numbers formed by the H-shaped copolymers. However, the case of dendritic−star copolymers with a non-bell-shaped distribution of aggregates is different. Aggregates with small aggregation number form spherical micelles (Figure 6c), while those with higher N_p form rod-like or worm-like micelles.

Figure 6. Snapshots of micelles formed by (a) $D_3G_2S_1(B_{10})_3$ with $N_p = 21$, (b) the same as shot a, but the two aggregative domains of one copolymer chain, bridging two smaller micelles, are colored yellow to guide the eye, and (c) $D_2G_2S_3(B_{30})_1$ with $N_p = 14$.

The reason is that the units of the two or three solvopholic linear arms can be concentrated in one, two, or three aggregative domains, and therefore nonspherical micelles can be formed.

In Figure 6a, a worm-like micelle is illustrated. The same micelle is depicted in Figure 6b, but the two aggregative domains of one copolymer chain, bridging two smaller micelles, are colored yellow to guide the eye. Similar nonspherical micelles, as we already mentioned in the Introduction, are also formed from star block copolymers[14] in dilute solution and in star polymers attached to nanospheres in more concentrated solutions.[24] The formation of aggregative domains in dendritic−star copolymers with two or three solvophobic arms depends on the number of solvophilic

dendrons and on their molecular weight. The higher the number of dendrons, the higher the density of the solvophilic core. In this situation, the solvophobic units are exposed in the periphery of the dendron, creating one or more aggregative points. Indeed, in the case of dendritic−star copolymers with $r = 1.36$, the ones with one dendritic arm $D_1G_2S_3(B_{10})_3$ form spherical micelles with preferential aggregation number. This happens because the solvophobic units can be concentrated all together in the free available space in the interior of the copolymer molecule while the other with three solvophilic and three solvophobic arms $D_3G_2S_1(B_{10})_3$ form micelles with wide aggregation numbers both spherical and nonspherical.

From the scaling theory point of view, three types of micelles are defined[25] on the basis of the relative size of their core radius

(24) Cheng, L.; Cao, D. *J. Phys. Chem. C* **2010**, *114*, 5732–5740.

R_c with respect to the corona thickness H. A micelle has a star-like shape when $H \gg R_c$. The micelle has a crew-cut shape when the radius of the core is much larger than the thickness of the corona ($R_c \gg H$), while in other cases the micelle has an intermediate shape. The radius of the core R_c can be calculated from its mean square radius of gyration by the following relation: $R_{gcore}^2 = (3/5)R_c^2$. Similarly, the thickness of the corona H can be obtained as the difference of the radii of the whole micelle and the core ($H = R_{mic} - R_c$). Our results on the shape of the most probable micelles for the dendritic—star copolymers are listed in Table 2. It can be observed that the copolymers with small molecular weight ($M_w = 52$) form crew-cut micelles, while the other with $M_w = 73$ forms intermediate type micelles.

Conclusions

The micellization behavior of amphiphilic hybrid dendritic—star copolymers containing up to three solvophilic dendritic arms and one, two, or three solvophobic linear branches was studied with Brownian dynamics simulations. For copolymers with the same total molecular weight and solvophobic/solvophilic ratio r, we found that the cmc values of hybrid dendritic—star copolymers with one solvophilic dendritic arm are proportional to the number of linear arms. The cmc also increases with the increase of the number of dendritic branches. The linear diblock copolymers have the lowest cmc values in comparison with the respective ones of hybrid dendritic—star copolymers. Between copolymers with different architecture, the preferential aggregation number follows the inequality $N_{p\,\text{linear A15B30}} > N_{p\,\text{linear—dendritic D1G2S2 B30}} > N_{p\,\text{linear—dendritic D1G3S1B30}} > N_{p\,\text{dendritic—star D2G2S1B30}} > N_{p\,\text{star (A4)4B30}} > N_{p\,\text{dendritic—linear—dendritic D1G2S1(B30)D1G2S1}} > N_{p\,\text{H-shaped (A4)2B30(A4)2}}$ reflecting the difference in steric interactions between solvophilic units in the corona and the change in the free energy g_{pack}, associated with constraining the end or both of the solvophobic parts to lie on the periphery of the micelle core. The simultaneous increase of the number of dendritic and linear arms leads the formation of micelles with widely distributed aggregation numbers. Aggregates with small aggregation number form spherical micelles, while those with higher N_p form worm-like micelles. The reason is that the units of the two or three solvophobic linear arms, in the latter case, can be concentrated in one, two, or three aggregative domains, and therefore nonspherical micelles can be formed.

(25) Iatrou, H.; Willner, L.; Hadjichristidis, N.; Halperin, A.; Richter, D. *Macromolecules* **1996**, *29*, 581–591.